Numerical Study of Natural Ventilation in a Building using CFD Analysis

RANDY S. LAGUMBAY

Abstract

A Computational Fluid Dynamics (CFD) analysis of the air temperature distribution, airflow pattern and particle tracks in a naturally ventilated building is conducted. The effect of changing the boundary condition to the air temperature field and air movement is studied. The commercial software like CFX 5.4.1 is used in the simulation and analysis of the physical model problem. Results show that changing the boundary condition will affect the air temperature distribution and air movement inside a building. The accuracy of the solution will depend on the accuracy of the wall boundary condition value.

Introduction

*T*he determination of the pattern of airflow and the distribution of air temperature and pollutants within an enclosed space are very important. It is very useful in checking the performance of a ventilation system, verifying the comfort conditions, predicting thermal transport and smoke and fire spread predictions. Jones (1997) predict the air flow paths in naturally ventilated spaces, and the results indicate that CFD prediction is sufficiently accurate as compared to measured data.

RANDY S. LAGUMBAY, Instructor, College of Engineering, MSU-Iligan Institute of Technology, Iligan City, Philippines, Master of Engineering Science with specialization in Computational Fluid Dynamics (CFD) (2001) from The University of New South Wales, Sydney, Australia.

CFD has the capacity to model and simulate physical fluid phenomena such as air movement and air temperature distribution inside a building that cannot be easily measured with a physical experiment, with lower cost and more rapidly than with experimental procedures.

The development of the idea of using a computer to solve problems of the mechanics of fluid leads to the formulation of the Computational Fluid Dynamics (CFD). CFD is defined as "the science of determining a numerical solution to the governing equations of fluid flow whilst advancing the solution through space or time to obtain a numerical description of complete flow field of interest by means of computer-based simulation" [Elliott, (March 2000, What is cfd.html)].

The process of performing a CFD simulation is divided into three components such as pre-processing (setting up the simulation), solver (solving for the flow field), and post-processing (visualizing the results). In pre-processing, the geometry of the region of interest is defined. The boundary condition and properties of the fluid are specified. The type of a physical model needed in the simulation is selected and the control volume mesh is generated.

The solver integrates the governing partial differential equations over the entire control volumes in the regions, and converts a system of algebraic equations by generating a set of approximations for the terms in the integral equations.

In post-processing, the solutions obtained are visualized and analyzed. Visualization includes vectors plot, surface plot of the fluid properties such as temperature, pressure, velocity, etc.

The main objective of this research is to study numerically the behaviour of fluid flow such as the pattern of airflow and air temperature distribution in a naturally ventilated building. The CFD package such as CFX 5.4.1 is used in this project. CFX 5.4 is a finite volume technique, which subdivides the region of interest into small sub-regions, called control volumes.

The k-ε turbulent model is used in the experiment. This turbulent model is suitable for predicting steady flow fields. Launder and Spalding (1972) suggested that k-ε model is better as compared to large-eddy simulation model as confirmed by Rodi (1986)

II. Basic Concept on Natural Ventilation

Natural ventilation is energy efficient (i.e. no need of a mechanical system). It can be easily integrated into buildings and it provides a healthier and more comfortable environment if integrated correctly [Liddament (1996)]. It is suitable for many types of buildings such as low-rise dwellings, schools, small or medium–sized offices, recreation and public buildings in moderate or mild climates. It is very cost–effective compared with the capital, maintenance and operational costs of mechanical systems.

The achievement of an acceptable indoor air quality in the natural ventilation is based on the supply of fresh air to a space and the dilution of the indoor pollution concentration [Liddament (1990)]. The amount of supply air needed to ensure an acceptable indoor air quality depends on the amount and nature of the dominant pollutant source in space. In a naturally ventilated building, the total energy consumption will only depend on the season (either heating or cooling) and the occupant behaviour such as opening or closing the windows and doors.

Human thermal comfort is the condition in which an occupant feels comfortable in either a warmer or cooler environment. There are many parameters that can influence the overall comfort.

1. *Physical Parameters* – these include the air temperature distribution and thermal conditions of the environment, the relative humidity of the air, the local air velocity (mean and turbulent), the odours, the colours of the surroundings, the light intensity and the level of noise.
2. *Physiological Parameters* – these include the age, sex and specific characteristics of the occupants.
3. *External Parameters* – these include the occupant activities, clothing and social conditions.

Among these parameters, the local environment, represented by the dry bulb temperature, humidity and air velocity plays a significant role in thermal comfort. Air movement determines the convective heat mass exchange of the human body with the surrounding air. The modification of the air movement around the human body can help control the thermal comfort level. This can be done through variation of the inlet and outlet boundary conditions. In natural ventilation, the thermal comfort zone can shift to regions of

higher air temperatures. Moreover, Allard recommended that the maximum limit of indoor air movement is usually 0.8 m/s [Allard (1998)].

III. Physical Problem Formulation

Figure 3.1 shows the geometry of the library building illustrating the surface regions. Figure 3.2 shows the plan view of the model illustrating the internal solid regions. The specifications of the boundary conditions differ on every scenario.
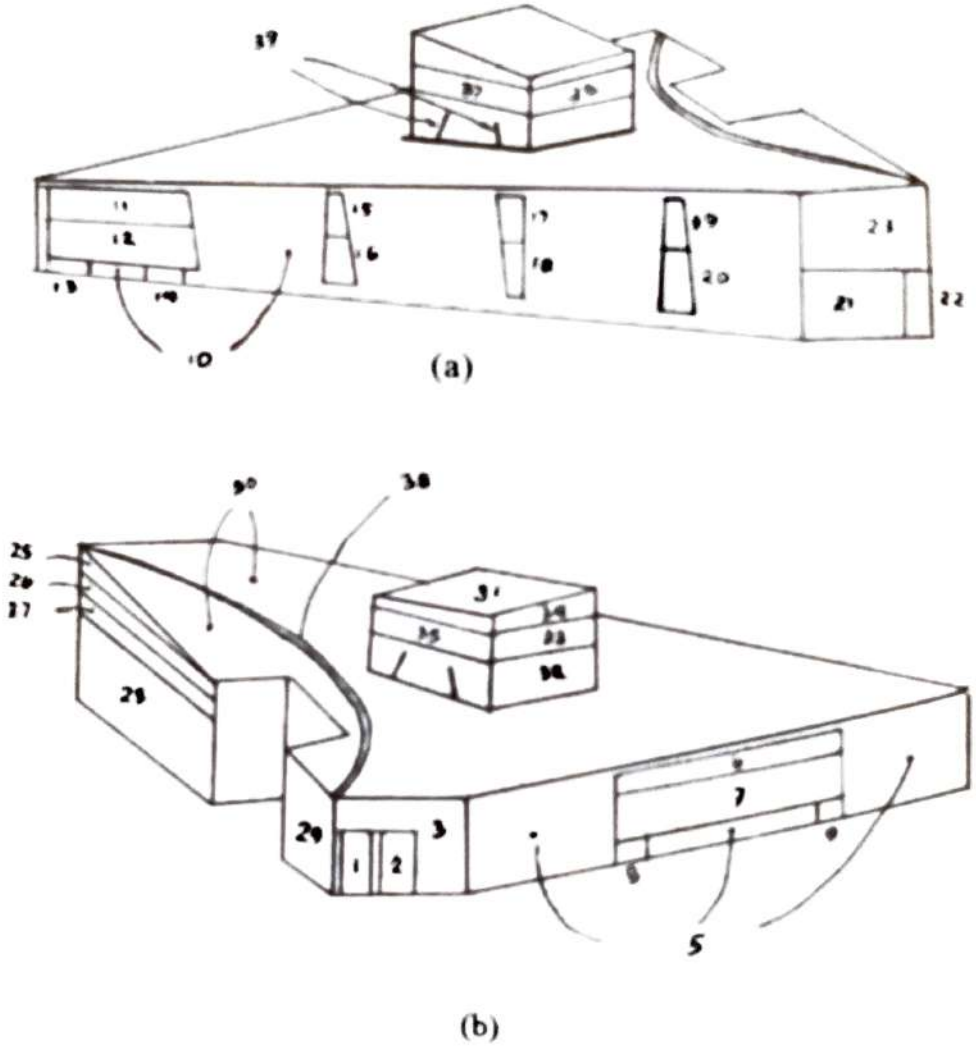

(a)

(b)

Figure 3.1. Geometry of the Physical Model Showing the Surface Regions. (a) Iso-2 View, (b) Iso-4 View.
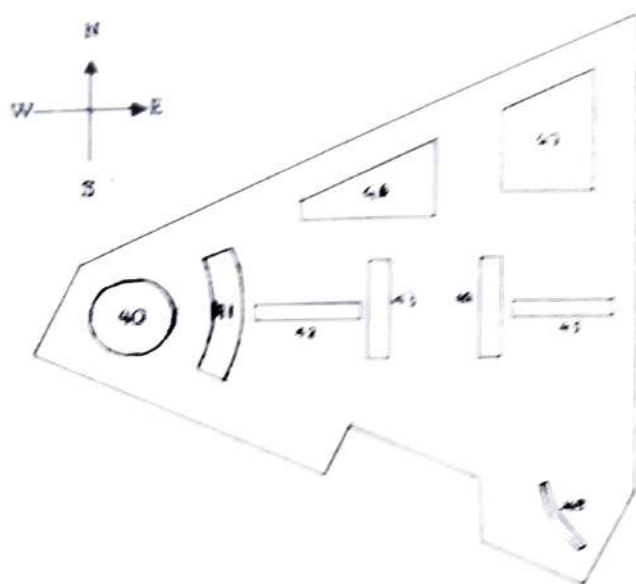
Figure 3.2. Plan View of the Physical Model Illustrating Internal Solid
Regions

IV. Mathematical Model and Solution Algorithm

The conservative form of the model equations that govern the time-
dependent three-dimensional fluid flow, heat and mass transfer of a com-
pressible Newtonian fluid are written as follows.

4.1 Governing Equations

The Continuity Equation:

$$\frac{\partial \rho}{\partial t} + \nabla \bullet (\rho U) = 0$$

The Momentum Equation:

$$\frac{\partial \rho U}{\partial t} + \nabla \bullet (\rho U \otimes U) = \nabla \bullet \left\{ -p\delta + \mu \left[\nabla U + (\nabla U)^T \right] \right\} + S_M$$

The Energy Equation:

$$\frac{\partial \rho h_{tot}}{\partial t} - \frac{\partial p}{\partial t} + \nabla \bullet (\rho U h_{tot}) = \nabla \bullet (\lambda \nabla T) + S_E$$

Where:

h_{tot} = is the specific total enthalpy expressed in terms of the specific static (thermodynamic) enthalpy, h. $h = h (P, T)$

h_{tot} = $h + \frac{1}{2} u^2$

The transport equation for an additional variable (non-reacting scalar) in the presence of turbulence:

$$\frac{\partial \phi}{\partial t} + \nabla \bullet (U\phi) - \nabla \bullet \left\{ \left(\rho D_\phi + \frac{\mu_t}{Sc_t} \right) \nabla \bullet \left(\frac{\phi}{\rho} \right) \right\} = S_\phi$$

Where,

ρ = mixture density, mass per unit volume.

ϕ = conserved quantity per unit volume, or concentration

$\frac{\phi}{\rho}$ = conserved quantity per unit mass

S_ϕ = volumetric source term, with units of conserved quantity per unit   volume per unit time.

D_ϕ = kinematic diffusivity for the scalar

μ_t = turbulence viscosity, with Sct the turbulence Schmidt number

Energy Sources: $S_E = S_{spec,E} + C_E T$

The energy sources can be specified within sub-domains in terms of a specified source value, $S_{spec,E}$ and a linear source coefficient, C_g.

4.2. The k-ε model.

The eddy viscosity hypothesis for the turbulence is applied in this model. There are two new variables being introduced into the system of equations.

k = is the turbulence kinetic energy defined as the variance of the fluctuations in velocity

ε = is the rate at which the velocity fluctuations dissipate.

The model equation for fluid flow, heat and mass transfer then becomes:

Continuity Equation:

$$\frac{\partial \rho}{\partial t} + \nabla \bullet (\rho U) = 0$$

Momentum Equation:

$$\frac{\partial \rho U}{\partial t} + \nabla \bullet (\rho U \otimes U) - \nabla \bullet (\mu_{eff} \nabla U) = \nabla p' + \nabla \bullet (\mu_{eff} \nabla U)^{Y} + B$$

Where,

B   = the sum of body forces
μeff   = the effective viscosity according to turbulence
P'   = the modified pressure given by $P' = P + \frac{2}{3}\rho k$

Since the k-ε model is based on the eddy viscosity concept, then

$$\mu_{eff} = \mu + \mu_t$$

where,

$$\mu_t = \text{turbulence viscosity}$$

$$\mu_t = c_\mu \rho \frac{k^2}{\varepsilon}$$

And, the transport equation for the turbulence kinetic energy and turbulence dissipation rate is given by:

$$\frac{\partial \rho k}{\partial t} + \nabla \bullet (\rho \mu k) - \nabla \bullet \left(\frac{\mu_{eff}}{\sigma_k} \nabla k \right) = P - \rho \varepsilon$$

$$\frac{\partial \rho \varepsilon}{\partial t} + \nabla \bullet (\rho \mu \varepsilon) - \nabla \bullet \left(\frac{\mu_{eff}}{\sigma_\varepsilon} \nabla_\varepsilon \right) = \frac{\varepsilon}{k} \left(C_{\varepsilon 1} P - C_{\varepsilon 2} \rho \varepsilon \right)$$

· where:

$C_{\varepsilon 1}, C_{\varepsilon 2}, \sigma_k, \sigma_\varepsilon$ are dimensionless constant.

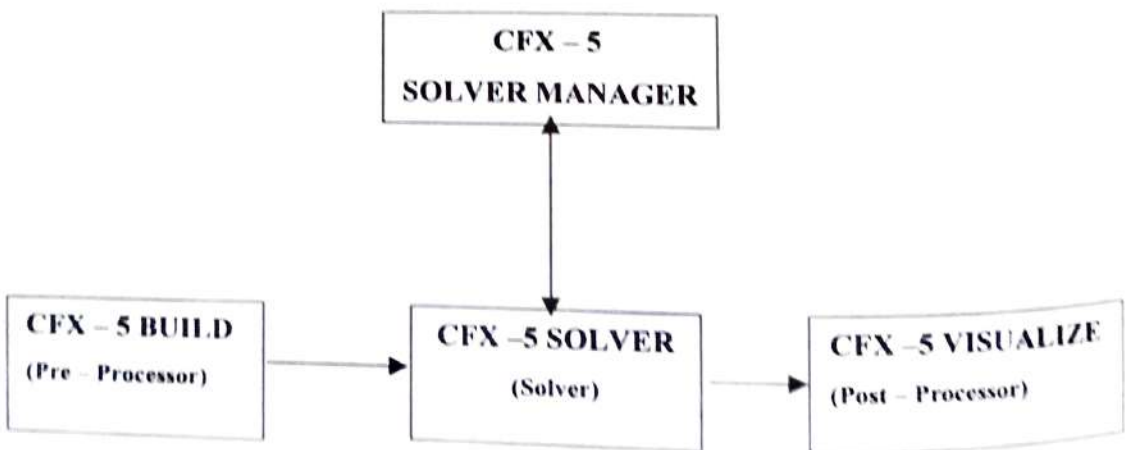|	
$C_{\varepsilon 1}$ = 1.44	σ_k = 1.0
$C_{\varepsilon 2}$ = 1.92	σ_ε = 1.3

P = the shear production due to turbulence, which for incompressible flow is given by,

$$P = \mu_t \nabla U \bullet \left(\nabla U + \nabla U^T \right) - \frac{2}{3} \nabla \bullet U \left(\mu_t \nabla \bullet U + \rho k \right)$$

V. CFD Analysis and Simulation using CFX 5.4.1

The process of performing a CFD analysis and simulation consists of four software modules which are connected by the flow of information required.

- ### CFX - 5 BUILD

This is the component where the CFD model is generated. It involves the following:

1. Defining the geometry of the region of interest.
2. Specifying the flow physics.
3. Specifying the boundary conditions.
4. Specifying the mesh parameters.
5. Setting the initial values and solver parameters.

- ### CFX - 5 SOLVER

This component solves all the solution variables for the particular simulation based on the problem specification generated. It uses a coupled solver that solves all the hydrodynamic equations as a single system.

- ### CFX - 5 SOLVER MANAGER

This component gives a greater control over the management of the CFD task, driven by a graphical user interface. This allows specifying the input files to the CFX - 5 Solver. The progress of the solutions towards convergence is monitored here.

- ### CFX - 5 VISUALIZE

CFX - 5 Visualize provides interactive graphic tools used to analyze and present the results from CFX - 5 simulations.
Some important features:

1. Visualization of the geometry and control volumes
2. Velocity vector and contour plots on arbitrary planes
3. Particle tracking
4. Iso-surfaces coloured with any variable
5. Coloured streamlines
6. Mesh visualization

7. Colour postcript output
8. Dynamic animation

5.1. Creating the Geometry of the Physical Model

Proen Design Australia Pty. Ltd provided the geometry of the physical model in an IGES format. A database is created with a global model tolerance of 0.01. Creating a B-rep solid representation, completes the geometry. A *B-rep* solid is defined by the surfaces enclosing a volume. A solid is needed to create a Fluid Domain for the simulation.

In this research, three scenarios are performed. For Scenario 1, only one solid is created. This is represented by the external surfaces of the building. This solid then defines the Fluid Domain region.

For Scenario 2 and Scenario 3, the solid block regions such as region 40 and 47 inside the building is considered as a conducting fluid sub-domain because these are assumed as a heat source. The external surfaces of the building are treated as the Fluid Domain region.

5.1.   Creating the Fluid Domain

The Fluid Domain defines the type, properties and regions of the flow. For the three cases, the Fluid Domain is the bounding solid represented by the external surfaces of the building. The fluid models used for the simulation are summarized below:

Reference Coordinate Frame = Coord 0
Reference Pressure   = 101.325 kPa
Simulation Type   = Steady State
Domain Motion   = Stationary
Available Fluid   = Air at STP
Turbulence Model   = k – epsilon
Heat Transfer Model   = Total Energy
Buoyancy Model   = Non-Buoyant

A steady state condition is assumed in this research so that time variation is not significant. However, this is not the usual case in actual situation. Also, k – epsilon model is used for the simulation because it is proven to be effective in predicting flow pattern and temperature field distribution for turbulent modeling around and inside a building [Sun and Huang (2001)].

5.2. Creating the Fluid Sub–Domain

A Fluid Sub–Domain is a solid region within a predefined Fluid Domain that can be used to specify values for volumetric sources of energy and momentum. For Scenario 2 and Scenario 3, the solid region, such as regions 40 and 47 inside the building, is defined as a volumetric heat source with a heat input of 1300 watts.

5.3. Specifying the Boundary Condition

The Navier–Stokes equation can be solved by specifying the conditions on the external boundary of the Fluid Domain. Hence, the boundary conditions determine the characteristics of the solutions obtained.

In this research, there are four types of boundary conditions such as inlet, outlet, opening and wall that are used. The boundary conditions vary for each scenario. The boundary condition is very important in obtaining a reliable and accurate solution. To compare the accuracy, the value of the heat transfer on the wall type boundary condition is evaluated using constant heat flux and heat transfer coefficient value of the wall.

VI. Results and Discussions

The results of the experiment show that the wall boundary condition can greatly affect the accuracy and reliability of the solution of the model flow problem, particularly in the air temperature distribution. It was found out that using heat transfer coefficient gives more reliable and accurate results as compared to constant heat flux for the wall boundary condition values. This is due to the influence of the heat transfer from the wall.

In addition, the movement of particles in ventilated areas is very compli-

cated. This is influenced by several factors, such as airflow patterns, particle properties, geometrical configurations, ventilation rates, supply and exhaust diffusers, thermal buoyancy due to the heat generated by occupants and/or equipment, etc.

6.1. Scenario 1

In this scenario, Celdek 35 is open for the outlet of air inside the room. All the windows are closed. Four small vents such as vents 8, 9, 13 and 14 are open. A mass flow rate of 4.86 kg/sec at 26.32 °C is supplied at the inlet celdek 37. Also, there is no generation of heat inside the building.

6.1.1. Using Heat Flux for the Wall Boundary Condition Value.

The results show that there is a big temperature difference inside the building. The maximum temperature is 872.014 [K] while the minimum temperature is 299.32 [K]. As can be seen, the maximum temperature is unrealistic. This is an abnormal temperature condition for a typical room air temperature. The normal air temperature for good thermal comfort of the occupants inside a building usually ranges from 27 °C to 32 °C dry bulb temperature. The increase of the temperature inside the building is due to the fact that the wall boundary condition value is set to constant heat flux, which causes a constant pumping of heat when the simulation is set to steady state.

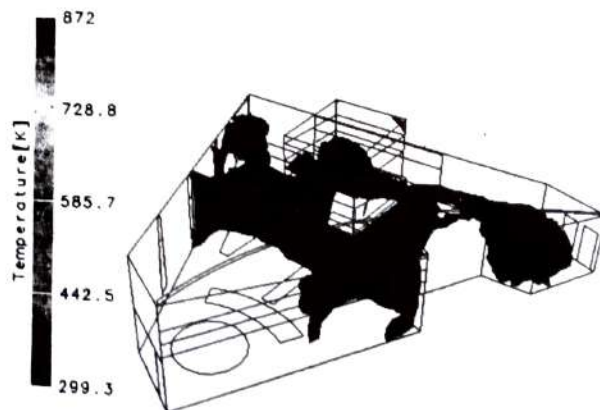### (a). Air Temperature Distribution

Figure 6.1.1.1. Iso-surface Plot of the 32 °C Dry Bulb Temperature. (Result using constant heat flux for the wall boundary condition value)
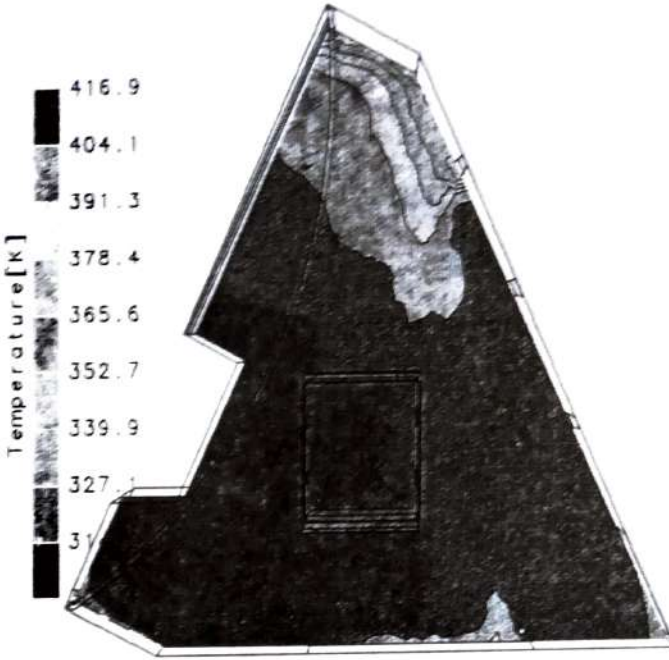
Figure 6.1.1.2. *Surface and Contour Plot of Dry Bulb Temperature at 2 Meters Height. (Result using constant heat flux for the wall boundary condition value)*
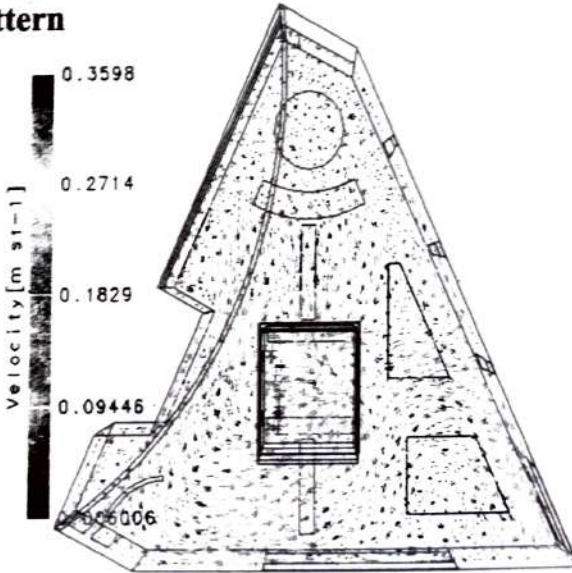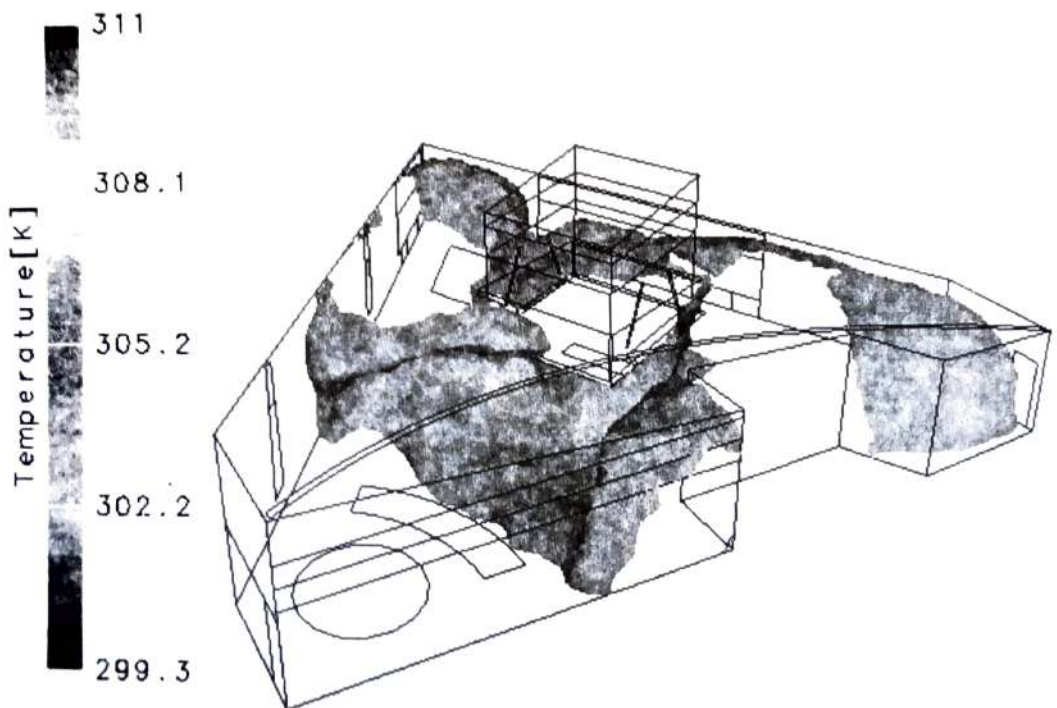
(b) Air flow pattern

Figure 6.1.1.3. *Plot of Velocity Vectors at 2 Meters Height. (Results using constant heat flux for the wall boundary condition value)*

6.1.2. Using Heat Transfer Coefficient for the Wall Boundary Condition Value

The solutions obtained are more accurate and reliable as compared to the previous solution using constant heat flux for the wall boundary condition value. Results show an improvement of the temperature inside the building. It can be seen that the maximum temperature reduces to 311 [K], which gives a reliable temperature range inside a building. The use of constant heat flux for the wall boundary condition value over-estimates the temperature due to the continuous pumping of heat inside the building. Thus, for steady state simulation, the wall boundary condition value must be set to heat transfer coefficient to prevent constant pumping of heat inside the building.

(a) Air temperature distribution

Figure 6.1.2.1. *Iso-Surface Plot of the 32 °C Dry Bulb Temperature. (Result using heat transfer coefficient for the wall boundary condition value)*
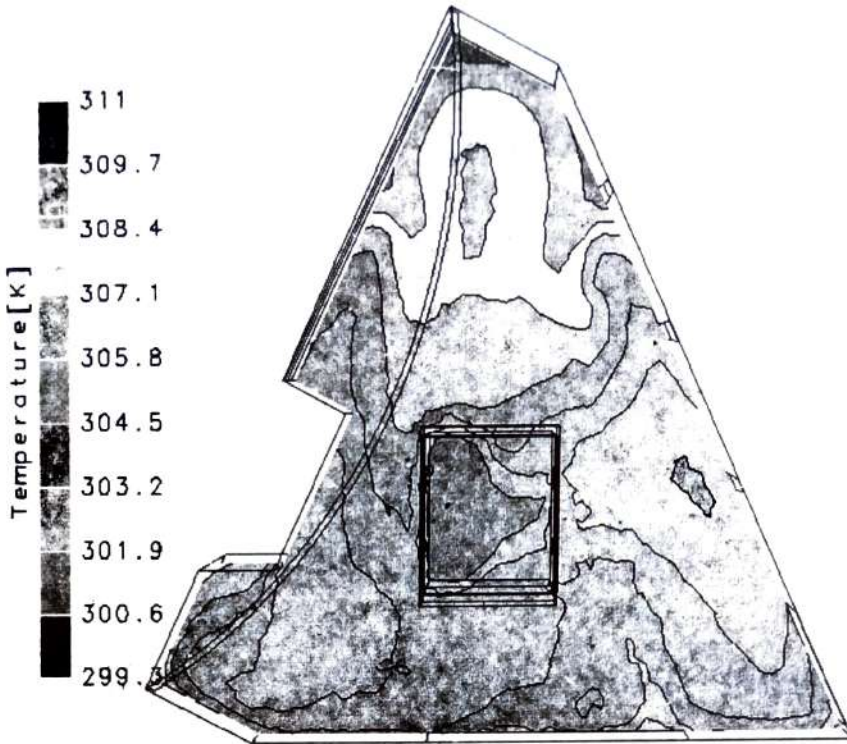
Figure 6.1.2.2. *Surface and Contour Plot of Dry Bulb Temperature at 2 Meters Height. (Result using heat transfer coefficient for the wall boundary condition value)*
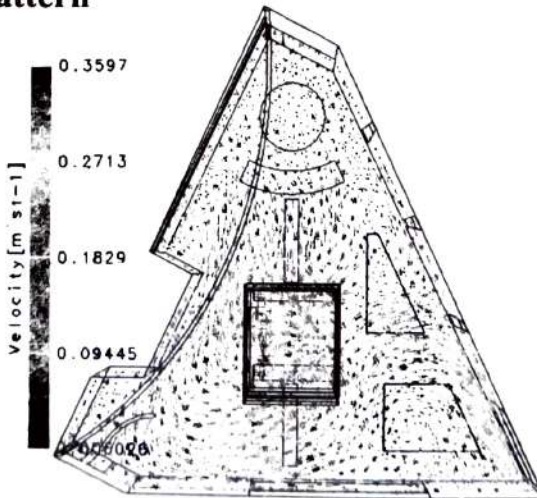
(b). Air Flow Pattern

Figure 6.1.2.3. *Plot of Velocity Vectors at 2 Meters Height. (Result using heat transfer coefficient for the wall boundary condition value)*

6.2. Scenario 2

The air temperature distribution and airflow pattern can be improved by varying the opening boundary condition. In this scenario, the outlet celdek 35 is closed. However, the four big windows such as windows 6, 11, 23 and 26 are open aside from the four small vents. Results show that there is an improvement of the air temperature distribution and airflow pattern in the occupant zone. The opening of the four big windows helps to even the distribution and mixing of supply air stream to the room air.

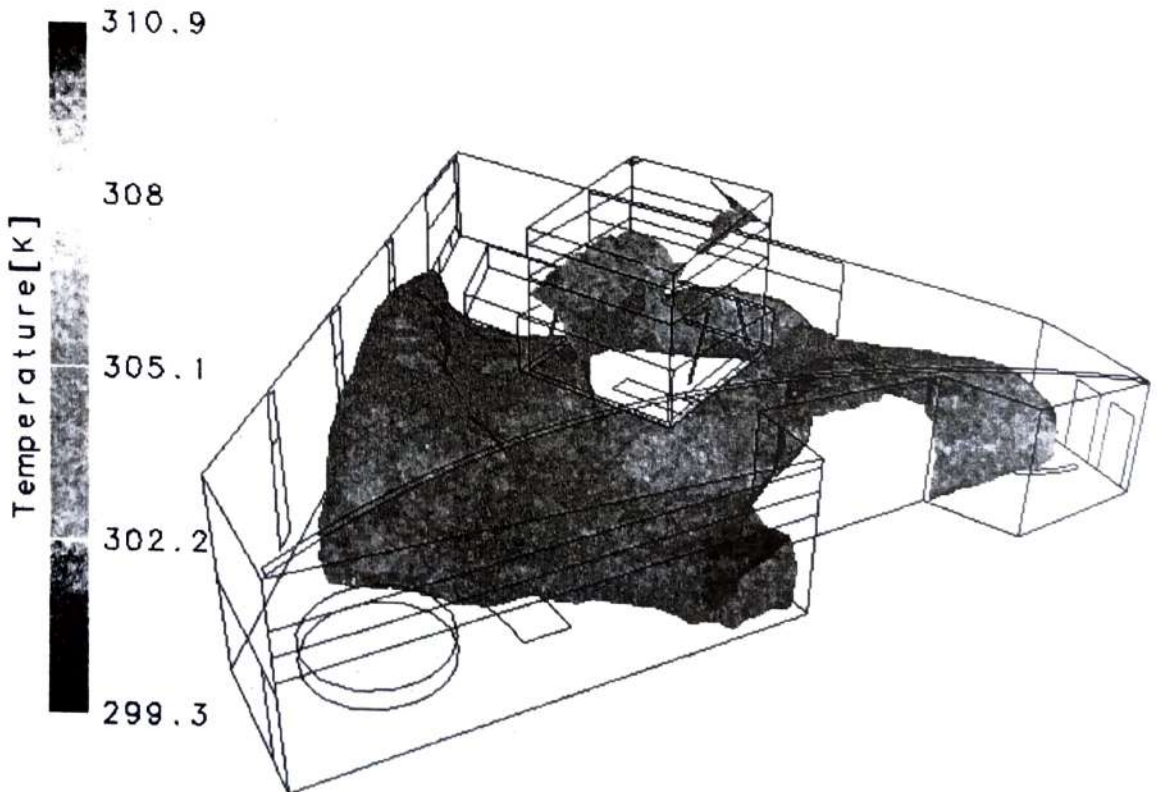### 6.2.1. Air Temperature Distribution

Figure 6.2.1. *Iso-Surface Plot of the 28 °C Dry Bulb Temperature. (Scenario 2)*
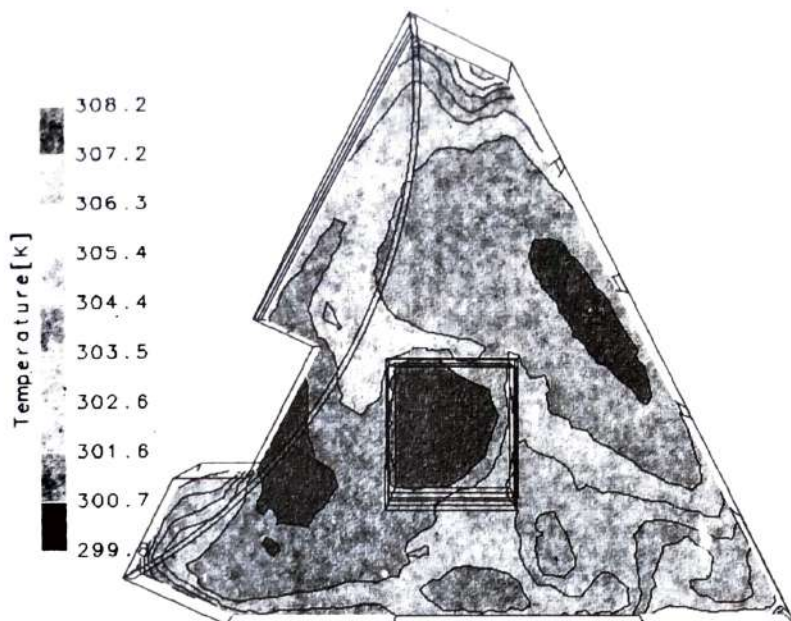
Figure 6.2.2. *Surface and Contour Plot of Dry Bulb Temperature at 2 Meters Height. (Scenario 2)*

6.2.2. Air Flow Pattern

The airflow pattern varies significantly due to the changes of the outlet and opening boundary condition. Results show a good airflow distribution on the occupants zone with a speed ranges from 0.1 m/sec to 0.3 m/sec.

At 2 meters height, air re-circulates near the lower side of the celdek due to the thermal buoyancy and airflow pattern of the supply air stream. A low air speed occurs near the heat source region due to the meeting of convective current of supply air stream and the thermal buoyancy due to the heat source. Near the sidewall, a " creeping " flow occurs moving directly towards the open window.
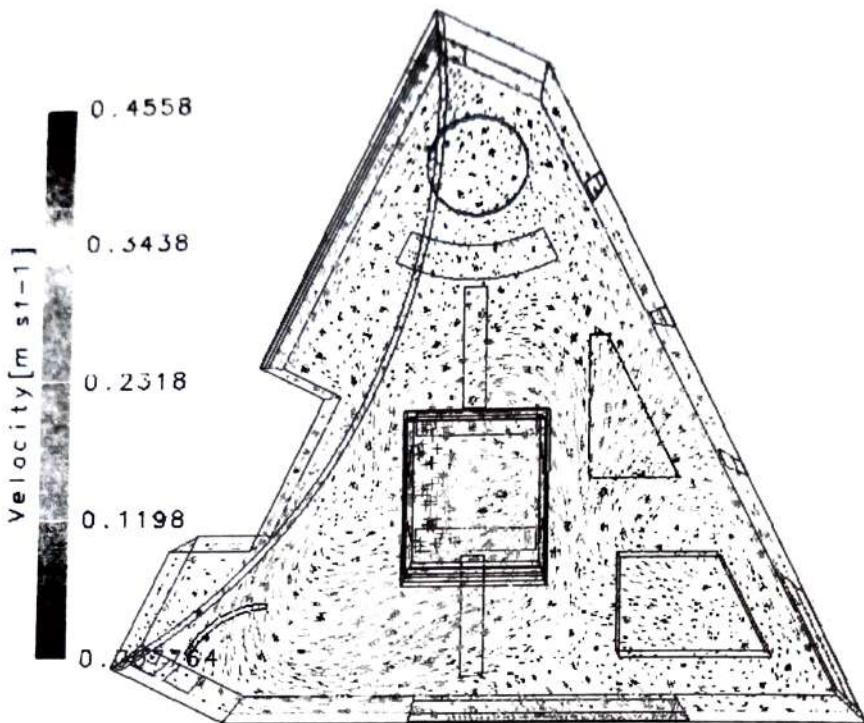
Figure 6.2.3. Plot of Velocity Vectors at 2 Meters Height. (Scenario 2)

6.3. Scenario 3

This is very similar to Scenario 2 except that the four small vents such as vents 8, 9, 13 and 14 are closed. Most of the boundary conditions are the same. The solution presented is the result of using heat transfer coefficient due to the accuracy as compared to constant heat flux for the wall boundary condition value.

6.3.1. Air Temperature Distribution

The maximum temperature inside the room is reduced by about 5 [K] as compared to Scenario 2. As can be seen in Figures 6.3.1, the temperature inside the building ranges from 299.3 [K] to 310.8 [K]. This is due to the fact that the entry of some hot outside air through the opening vent is reduced. This causes the reduction of mixing of cold supply air stream and hot outside air.
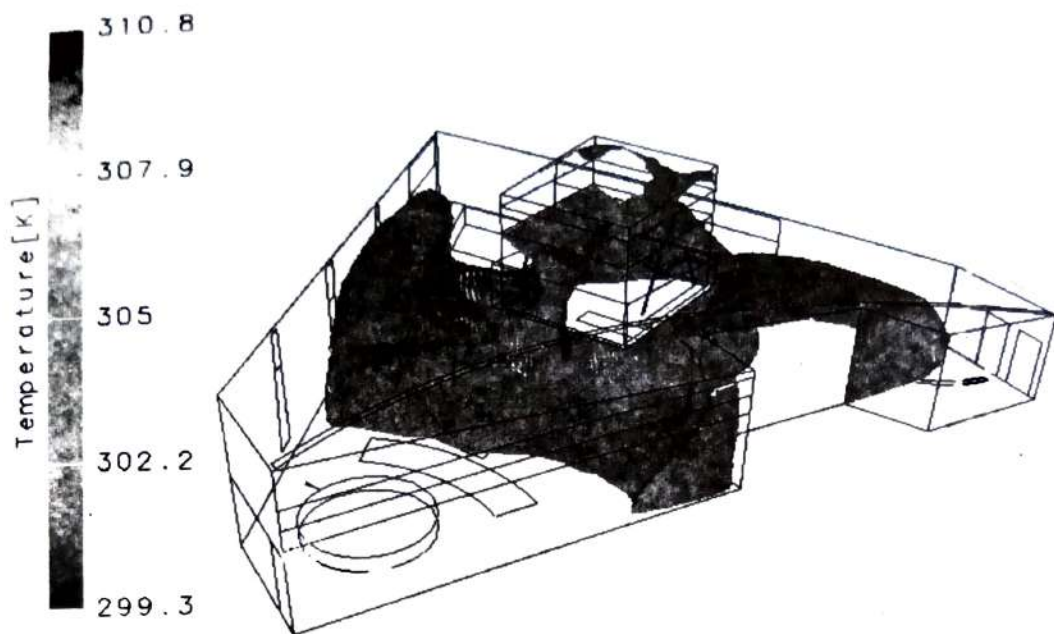
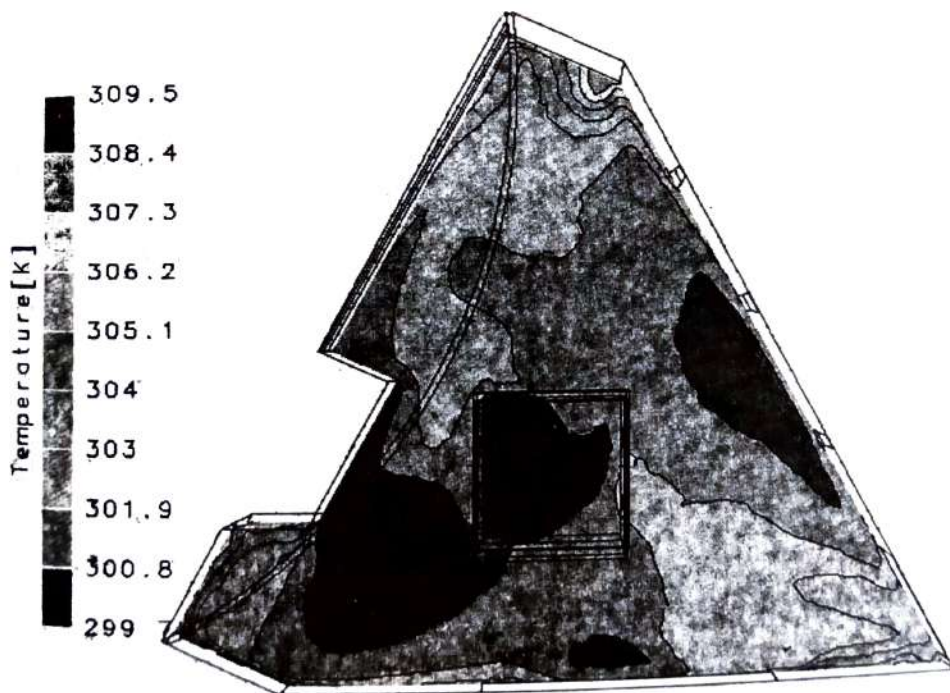**Figure 6.3.1.** *Iso-Surface Plot of the 28 °C Dry Bulb Temperature. (Scenario 3)*

Figure 6.3.2. *Surface and Contour Plot of Dry Bulb Temperature at 2 Meters Height. (Scenario 3)*
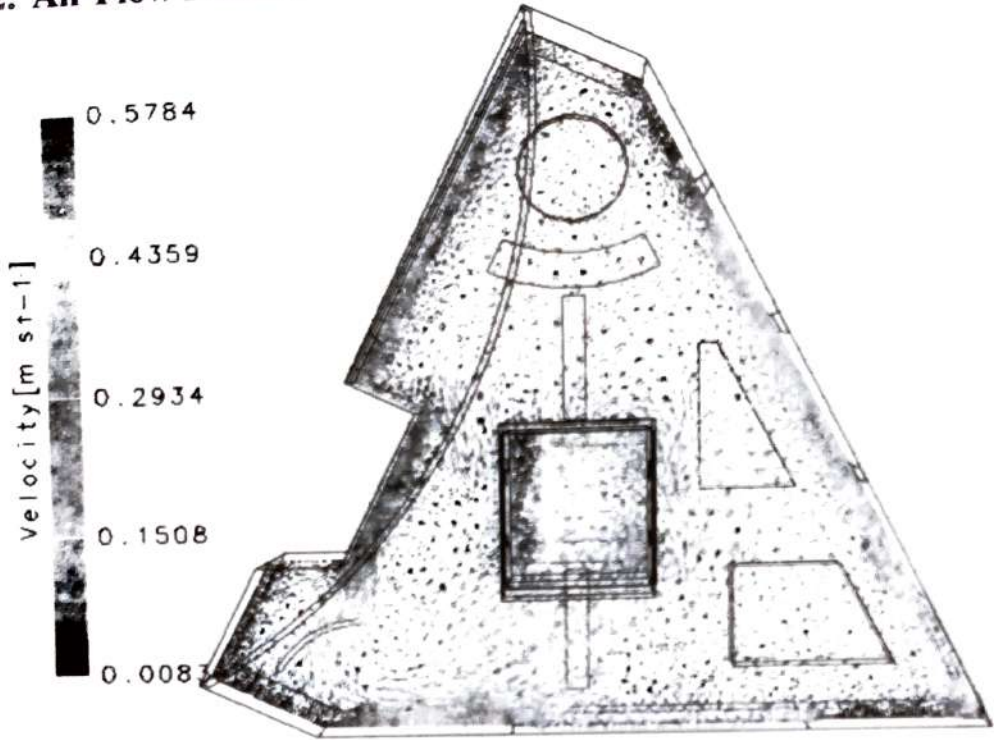
6.3.2. Air Flow Pattern

Figure 6.3.3. Plot of Velocity Vectors at 2 Meters Height. (Scenario 3)

6.3.3. Particle Tracks

There are six particles released at the same location of Scenario 2. Results show that closing the four small vents can greatly affect the particles movement. Most of the particles move directly towards the open windows on the west side of the building due to the pattern of the supply air stream, thermal buoyancy and closure of the four small vents. Instead of moving the air through the vents, it bounces back through the space and moves through the other side driven by the airflow pattern of the supply air stream and thermal buoyancy. The particles move with a complex spiraling and mix at the central space.
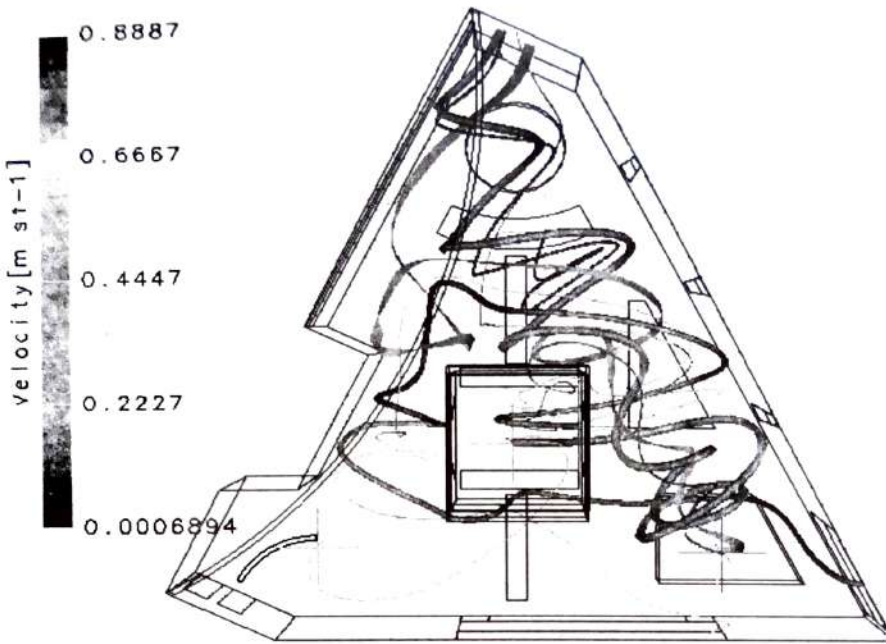
Figure 6.3.4.   *Top View. Particle Tracks of Six Small Negligible Mass Particles Placed at Different Locations. (Scenario 3)*

VII. Conclusions and Recommendations

The CFD technique using a commercial CFD package like CFX 5.4.1 was used in the numerical study of a naturally ventilated building. In most design of ventilation, the main concern was the thermal comfort condition of the occupants. The physical factors play a significant role in satisfying the thermal comfort condition of the occupants. This includes the air temperature distribution, airflow pattern and pollutants distribution inside the building.

A three dimensional simulation using CFX 5.4.1 was conducted in the experiments. The physical model is a library building provided by Proen Design Australia Pty. Ltd. There were three scenarios performed by simply varying the boundary conditions. Based on the results presented, the following conclusions can be deduced:

1. The CFD analysis provides a good approximation of the solution of the Navier-Stoke equation. The accuracy depends on the accuracy of the boundary conditions value and grid refinement. The wall boundary condition values can affect the accuracy and reliability of the numerical solution. It was found out that the heat transfer coefficient provides a more accurate and reliable results as compared to constant heat flux in a steady state simulation. The result shows that the use of constant heat flux overestimates the maximum temperature inside the building. In addition, mesh refinement improves the accuracy of the numerical solution. A very fine mesh is more accurate compared to a coarse mesh. However, the computational cost is higher and convergence is more difficult to achieve.

2. The CFD package like CFX 5.4.1 has the capacity to simulate and predict the three dimensional distribution of airflow pattern, temperature and particle tracks. This is very useful in providing information when verifying whether the ventilation design for the building can provide a satisfactory environment for the thermal comfort of the occupants.

3. The variation of the outlet and opening boundary condition can affect greatly the airflow pattern and particle's movements. Moreover, the heat source inside the building, like in Scenarios 2 and 3, can affect the air temperature distribution, airflow pattern and particle's movement due to the thermal buoyancy effect.

4. The use of k-epsilon model provides better results.

Furthermore, in this research project, the outside temperature is assumed constant during the simulation. However, in actual situation, the temperature outside the building is affected by several factors such as the orientation of the building and wind movement. Thus, it is recommended to evaluate the results using a transient simulation for more realistic results.

List of Symbols

Symbol	Description	Dimensions
ρ	Density	ML^{-3}
δ	The Identity Matrix or Kronecker Delta Function	1
μ	Dynamic Viscosity	$ML^{-1}T^{-1}$
λ	Thermal Conductivity	$MLT^{-3}K\Theta^{-1}$
ϕ	Scalar Variable	
c_p	Specific Heat Capacity at Constant Pressure	$L^2T^{-2}\Theta^{-1}$
ε	Turbulence Dissipation Rate	L^2T^{-3}
μ_{eff}	Effective Viscosity, $\mu + \mu_t$	$ML^{-1}T^{-1}$
μ_t	Turbulent Viscosity	$ML^{-1}T^{-1}$
B	Sum of Body Forces	$ML^{-2}T^{-2}$
D_ϕ	Kinematic Diffusivity of an Additional Variable	L^2T^{-1}
h_{tot}	Specific Total Enthalpy	L^2T^{-2}
k	Turbulence Kinetic Energy per unit Mass	L^2T^{-2}
$\overset{\bullet}{m}$	Mass Flow Rate	MT^{-1}
p'	Modified Pressure	$ML^{-1}T^{-2}$
S_ϕ	Volumetric Source	$ML^{-3}T^{-1}$
S_{Ct}	Turbulence Schmidt Number, $c_p\mu_t/\lambda$	1
S_E	Energy Source	$ML^{-1}T^{-3}$
S_M	Momentum Source	$ML^{-3}T^{-2}$
T	Temperature	Θ
U	Velocity Vector	LT^{-1}

Source: CFX – 5 online manual

Acknowledgement

Above all, from the bottom of his heart, he offers his success to the ALMIGHY GOD for giving him the knowledge, guidance, courage and strength.

References

1. ASHRAE (1993), ASHRAE Handbook – Fundamentals, American Society of Heating, Refrigerating and Air-conditioning Engineers, Atlanta, GA.

2. Allard, Francis (1998), *Natural Ventilation in Buildings: A Design Handbook*, James and James Ltd., p.5.

3. Ambi, H.B. (1989), "Application of Computational Fluid Dynamics in Room Ventilation", *Building and Environment*, Vol. 24, pp.73 – 84.

4. Bjorn, E. and Nielsen, P.V., "CFD Simulations of Contaminant Transport Between Two Breathing Persons", *Dept. of Building Technology and Structural Engineering*, Aalborg University, DK-9000 Aalborg, Denmark.

5. Bjorn, E., et al, "Improvement of Thermal Comfort in a Naturally Ventilated Office", *Proceedings of 21 st AIVC Conference*, Steigenberger Kurhaus Hotel, Den Haag, Netherlands, 26 – 29th Sept. 2000.

6. Castro, I.P., et al. (1977). *Fluid Mech.*, 79(2), 307 – 355.

7. CFX – 5 Tutorial 14: "Conjugate Heat Transfer in a Process Heating Coil", *CFX-5 online manual*, pp.1-189 – 1-200.

8. CFX-5 Solver and Solver Manager: "Mathematical Models and Solution Algorithms", *CFX-5 online manual*, pp.2-54 – 2-98.

9. CFX-5 Tutorial 15: "Flow around a blunt body", *CFX-5 online manual*, pp.1-9 – 1-37.

10. Chow, W.K. (1996), "Application of Computational Fluid Dynamics in Building Services Engineering", *Building and Environment*, Vol. 31, No. 5, pp. 425 – 436.

11. Chow, W.K. (2001), "Numerical studies of airflows induced by mechanical ventilation and air-conditioning (MVAC) systems", *Applied Energy*, Vol. 68, pp. 135 – 159.

12. Chung K.C. and Lee, C.Y. (1996), "Predicting Air Flow and Thermal Comfort in an Indoor Environment under Different Air Diffusion Models", *Building and Environment*, Vol. 31, No.1, pp. 21 – 26.

13. F. Stella, et al (1993), "The Rayleigh-Benard problem in intermediate bounded domains", *J. Fluid Mech*, Vol. 254, pp. 375 – 400.

14. Jayamaha, S. E., et al (1996), "Measurement of the Heat Transfer Coefficient for Walls", *Building and Environment*, Vol. 31, No. 5, pp. 399 – 407.

15. Jones, Phil J. (1997) , " Natural Ventilation: Prediction, Measurement and Design", *Naturally Ventilated Buildings: Buildings for the senses, the economy and society*, E and FN Spon., pp.148 – 149.

16. Launder, B.E. and Spalding, J.L. (1972), "Mathematical Models for Turbulence", Academic Press, New York.

17. Liddament, M. (1990), " Ventilation and Building Sickness – a brief review", *Air Infiltration Review*, Vol. 11 No.3, pp. 4 – 6.

18. Liddament, M. (March 1996), *A Guide to Energy Efficient Ventilation*, Air Infiltration and Ventilation Centre, Coventry, U.K., p. 69 – 86.

19. Lu, W., et al (1996), "Modelling and Measurement of Airflow and Aerosol Particle Distribution in a Ventilated Two-Zone Chamber", *Building and Environment*, Vol. 31, No. 5, pp. 417 – 423.

20. Martin, A.J (1995)., *Control of Natural Ventilation*, Tech. Note 11/95, BSRIA.

21. Murakami, S., and Kato S. (1989), "Numerical and Experimental Study on Room Airflow: 3 – D Predictions Using k – turbulence model", *Building and Environment*, Vol. 24, pp. 85 – 97.

22. Murakami, S., et al. (1992). *J. Wing Eng. Ind. Aerodyn*. 41 – 44, 2841 – 2852.

23. Rodi, W. (1986), *Trans. Am. Soc. Mech. Eng.*, Vol. 108, pp. 174-179.

24. Staples, P.D. (March 2000), *Fluent Inc. CFD Applications*, [http://www.fluent.com/applicat./applicat. Html] acc. 22 March 2000.

25. Sun, Heng and Huang, Suyi (2001), " Simulation of Wind Flow Around a Building with a k-ε Model ", *Theoretical and Computational Fluid Dynamics*, Springer – Verlag, Vol. 14 No.4, pp. 283 – 292.

26. Sutrisno (2000), " *Numerical Modelling of Concentration Levels in Car Passenger Compartment*", A thesis report on the School of Mechanical and Manufacturing Engineering, The University of New South Wales.

27. Troyak, Alex (2000), *"Natural Convection in Partially Closed Box"*, A thesis report on the School of Mechanical and Manufacturing Engineering, The University of New South Wales.

28. Versteeg, H.K. and Malalasekera, W. (1995), *An Introduction to Computational Fluid Dynamics: The Finite Volume Method*, Lingman Group Ltd, London.

29. Wong, K. Y., *"CFD Analysis of Temperature Fields Around a Residential Building results from Condensing Units Heat Rejection "*, A thesis report on the School of Mechanical and Manufacturing Engineering, The University of New South Wales.